Seasonal Snow Monitoring in Northeast China Using Space-borne Sensors: Preliminary Results

Kaishan Song[1], Yuanzhi Zhang[2], Cui Jin[1], Su Yan[2], Long S. Chiu[2]

[1]Northeast Institute of Geography and Agroecology, CAS
E-mail: songks@neigae.ac.cn
[2]Institute of Space and Earth Information Science, Chinese University of Hong Kong, HKSAR
E-mail: yuanzhizhang@cuhk.edu.hk

Abstract
Snow and meteorological measurements collected at six sites in Northeast China were used to compare snow cover area (SCA) retrieved from the Moderate Resolution Imaging SpectroRadiometer (MODIS) and QuikSCAT and snow water equivalent (SWE) retrieved from the Advanced Microwave Scanning Radiometer (AMSR). The SCA retrieved from QuikSCAT and MODIS are in qualitative agreement with each other and with in situ measurements. Based on in situ data from stations Qingyu and Dehui, SWE retrieved from AMSR show a bias of 43% and a R^2 value of 0.91 with in situ data for the early snow season. These results are consistent with previous estimates and point to the need to properly account for other snow properties such as snow density profile and grain size in the retrieval of regional snow parameters in Northeast China.
Keywords
space-borne data, snow covered area (SCA), snow water equivalent (SWE)

I. INTRODUCTION

Information on seasonal snow cover is crucial to water resource management, hydrological processes and climate in the boreal zone. Monitoring snow covered area (SCA) and snow water equivalent (SWE) at regional scale is essential for climate and hydrological applications. The maximum SWE prior to the onset of spring snowmelt is one of the most important snow characteristics for operational hydrology and run-off and river discharge forecasts (Pulliainen, 2006; Liang, et al., 2008; Wang, et al., 2008). The polar regions are also sensitive to global warming, hence cryospheric variables, such as sea ice and snow are good indicators of climate change (Foster, et al., 2008a). Accurate SWE information, however, is still difficult to provided because the SWE information are usually obtained from either interpolating observations of gauging networks and snow courses or interpolating daily synoptic weather station-based point-wise snow depth (SD) and precipitation information (Pulliainen, 2006). In dry snow conditions, the SWE information can be obtained from satellite-based microwave radiometric observations.

Passive microwave remote sensing plays a major role in monitoring of SCA and SWE because of its all-weather capabilities. Microwave radiometers usually have coarse resolutions, so the data size of passive microwave data at the regional scale is small. In comparison, optical sensors can provide a comparatively finer spatial resolution for monitoring in cloud-free conditions. Optical remote sensing data such as the Advanced Very High Resolution Radiometer (AVHRR) (Koskinen, et al., 1999) and MODerate Resolution Imaging Spectroradiometer (MODIS) have been introduced to monitoring snow condition (Hall, et al., 2001; Tekeli, et al., 2005; Parajka and Bloschl, 2008). In shallow dry snow conditions, times series of C-Band SAR data can potentially provide high spatial resolution data for all-weather monitoring (Bernier and Fortin, 1998).

In China, Terra/MODIS data have been applied to investigate snow cover and snow properties in Xinjiang and the results have been compared with in situ observations during four winters in northern Xinjiang (Liang, et al., 2008; Wang, et al., 2008). In addition, a modified Chang's model was applied for snow monitoring in Tibet-Qinghai region (Chang, et al., 1987; Che, et al., 2004). However, few studies have focused in snow monitoring in Northeast China (Song and Zhang, 2008).

Snow parameters and meteorological conditions have been collected at six sites in Northeast China for the 2005–2006 and 2006–2007 winters. In this study, we present the preliminary results of comparing field measurements of snow parameters with data from the Ku-band SeaWinds sensor on board the QuikSCAT satellite and SWE estimated from Advanced Microwave Scanning Radiometer (AMSR-E) for December of 2005. The snow covered area (SCA) is compared with that retrieved from MODIS data.

Section II provides a description of the region, its climate and in situ and satellite data. Section III describes the results of comparison of daily observations of SWE and monthly SCA and SWE estimate with remote sensing estimates. SCA estimated from QuikSCAT and MODIS and SWE from AMSR are compared. Section IV summarizes our preliminary results and discusses future plan for analysis.

1082-4006/08/14(02)-113$5.00

II. STUDY AREA AND DATA COLLECTION

Northeast China is situated between 42° to 52° N and 106° to 134° E, with an area of 1, 240, 897 km^2 (Figure 1). Its elevation varies from 110m to 2760m. It is surrounded by Inner Mongolia to the west, Russia to the north and northeast and North Korea to the east. It is characterized by diverse land cover types, ranging from temperate evergreen conifer-deciduous broad leaf mixed forests, deciduous broad leaf forests, woodlands, and scrublands in the Changbai Mountain, the Daxing'an and Xiaoxing'an Mountain Ranges to typical steppes and desert steppes in the west, and agricultural lands (e.g., the Liao River Plain, the Songnen Plain and the Sanjiang Plain), meadow steppes in the middle.

Figure 1. The study area in Northeast China

The area has a temperate continental monsoon climate. The annual precipitation decreases gradually from the eastern mountainous region to the middle farmland and then to the western pastoral area. Temporal and spatial precipitation variability, such as annual inter-annual and intra-annual changes, is large. Air temperature spatially increases from south to north with a mean annual values of 2–6°C. Spatial climatic patterns in the region can be described by three important features: a predominantly north–south gradient in mean annual temperature (MAT) from less than 3°C in the north–west and in the north-east to 3–7°C in the middle; a predominantly west–east gradient in mean annual precipitation (MAP) from 100–300 mm in the west, 300–600 mm in the middle, and 600–1000 mm in the east; and a north–south gradient of mean annual potential evapotranspiration (MAPET) that ranges from 500–600 mm in the north to 600–700 mm in the south. Temporal climatic patterns, the intra seasonal and inner-annual variability, are also high. The highest temporal variability is in the driest and coldest portions of the region. The frost-free period of the study area is 130–165 days. In summer, the study area is humid and warm with rainfall decreased from Changbai Mountain of 800mm to Hunlubei'er 300mm.

We have collected ground-based measurements in six testing sites. The sites are listed in Table 1. The ground data include daily morning and afternoon air temperatures and precipitation. In addition, snow depth (SD), snow water equivalent (SWE), and snow grain size were measured. SWE were estimated via the snow density, which is determined by melting a snow column and dividing the melted water height by the snow column height.

Ku-band data over the region of Northeast China for the winter of 2005–2006 and 2006–2007 collected on board the QuikSCAT satellite are available from the website of QuikSCAT products (podaac-www.jpl.nasa.gov/**quikscat**). The dataset consists of horizontally and vertically polarized backscattering cross sections separately for ascending (morning) and descending (evening) orbits. The spatial resolution is about 22.5 km. The incidence angle is 46° for horizontally polarized channel and 54° for the vertically polarized channel. The sensor has a swath of 1800/1400 km (V/H polarization) allowing data acquisition for the region twice a day.

Passive microwave sensors have been used to retrieve snow water equivalent (Chang et al., 1982, Foster et al., 2008b, Nghiem et al., 2008). A simple SWE algorithm is of the form

$$SWE = a(T_{19} - T_{37}) - b \quad (1)$$

where a and b are empirical coefficients and T_{19} & T_{37} are the brightness temperatures at 19GHz and 37GHz vertical polarizations, respectively. The coefficient, a, shows large spatial and temporal variations and is dependent on the snow grain size, snow density, morphology of the snowpack, and the land cover type (Rott and Nagler, 1994). This algorithm has been applied to operational microwave sensors. For global applications, a single value is used. Because the algorithm is used globally, it would be interesting to see its applicability to Northeast China. A global Level 3 Advanced Microwave Scanning Radiometer (AMSR) product is the SWE mapped to Equal Area Scalable Earth (EASE)-grid (Kelly, et al., 2004). The five day average SWE-E at 0.25° data is acquired for comparison with in situ data (available from NSIDC http://nsidc.org/data/docs/daac/ae_swe_ease-grids.gd.html)

In addition, the MODIS SCA data (available from MODIS web site http://modis.gsfc.nasa.gov) in cloud-free conditions are acquired. The monthly MODIS SCA maps is produced using a Normalized Difference Snow Index (NDSI) which takes advantage of the spectral characteristics of snow and ice surface in the visible and IR region of the spectrum. The NDSI is used with the Normalized Difference Vegetation Index (NDVI) to help classification in vegetated areas. At each pixel, the NDSI is computed at the 500m pixels. For the monthly SCA

product, the pixel is classified as snow cover if it is snow covered in any days of the month, even when the pixel may be snow free during the rest of the month (Hall, et al., 2001).

III. METHODS AND RESULTS

Table 1 shows the dry snowpack measurements in the winter of 2005–2006 and 2006–2007 for all six sites. Over the two winters, the snow depth varied between 0.3–31cm, SWE between 0.6–60.7mm, snow surface temperatures ranged from –35°C to –5°C (i.e., 238–268°K), and the mean grain-size ranges from 0.2–2.5mm for the stations. The criterion for dry snow was three consecutive days with the max daily air temperature below –5°C, with the data acquired on the third day. Stations Qingyu, Yichun and Muleng show SWE above 30mm; Honghe at 20.4 mm and Hailun at 12.7 mm. Dehui showed the lowest average SWE value of 4.2 mm.

Table 1. Summary of field measurements at six testing-sites in Northeastern China

Sites	T_{min}	T_{max}	D_{size}	SD(cm)	SWE(mm)	SWE mean(mm)
Dehui	–23°C	–5°C	0.6–1.5mm	0.3–9cm	0.6–16.6mm	4.2mm
Hailun	–27°C	–5°C	0.2–0.7mm	1–12cm	2–23.5mm	12.7mm
Qingyu	–29°C	–5°C	0.6–1.5mm	5.4–28.1cm	10.2–53.5mm	32.8mm
Muleng	–35°C	–6°C	0.5–1mm	8.5–23.5cm	18.2–50.4mm	30.9mm
Honghe	–22°C	–5°C	0.2–0.6mm	5.9–31cm	11.6–60.7mm	20.4mm
Yichun	–33°C	–5°C	1–2.5mm	11–22cm	26.7–53.5mm	32.8mm

Two stations, Qingyu and Dehui, were selected for our initial analysis since they show the highest and lowest accumulated SWE. They also show similar grain size characteristics.

Figure 2 and 3 show the time series of snow depth and morning and afternoon (Tmin and Tmax) surface temperature in Qingyu and Dehui after the first snow day in December 2005. It can be seen that all the daily temperature are below -10°C, indicating the absence of melting. There are more snow (snow depth is higher) in Qingyu than Dehui, probably due to the influence of its proximity to the ocean. The snow densities are 0.19 ± 0.03g cm^{-3} for Qingyu and 0.16±0.02 g cm^{-3} for Dehui for the snow days in December 2005. The snow densities are slightly higher before 24 December in Qingyu (0.22g cm^{-3}). The snow density is slightly more variable in Dehui.

AMSR estimates of SWE using the modified Chang et al. technique in the EASE grids that contains these stations are also plotted in these time series (shown in squares). The AMSR estimates are in general higher. Figure 4 shows the scatterplot

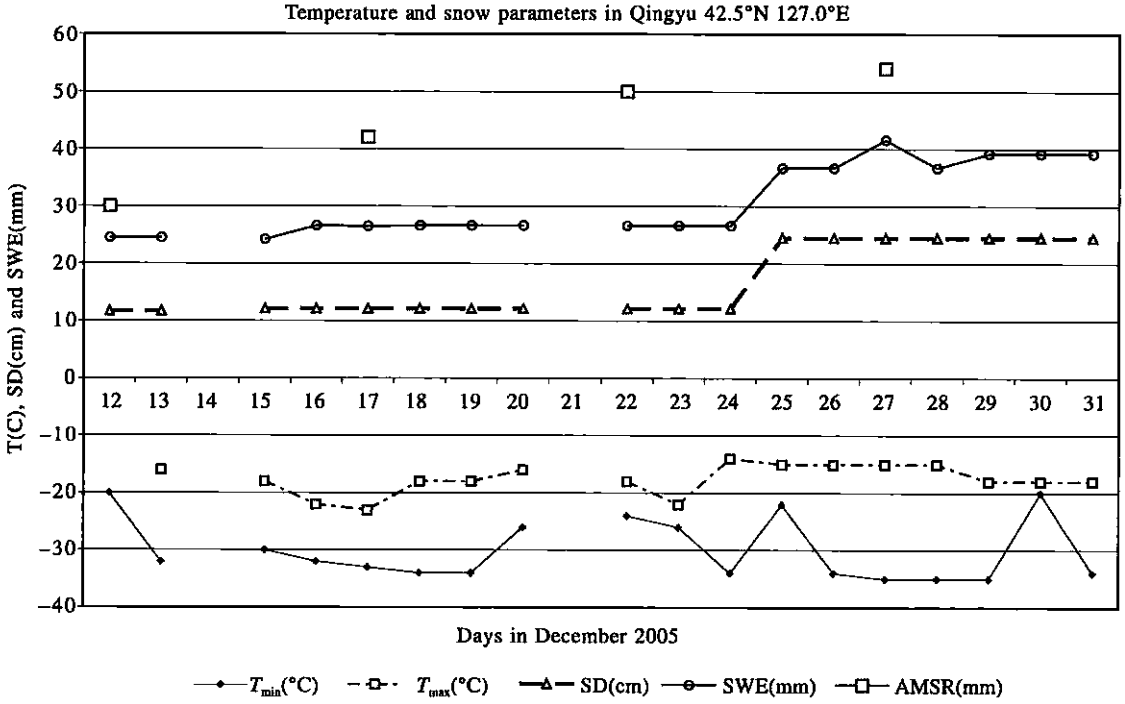

Figure 2. Time series of morning (Tmin), afternoon (Tmax) surface air temperature, snow depth (SD in cm) and snow water equivalent (SWE in mm) in station Qing Yu for December 2005. Data for 14 and 21 December (left blank) are missing

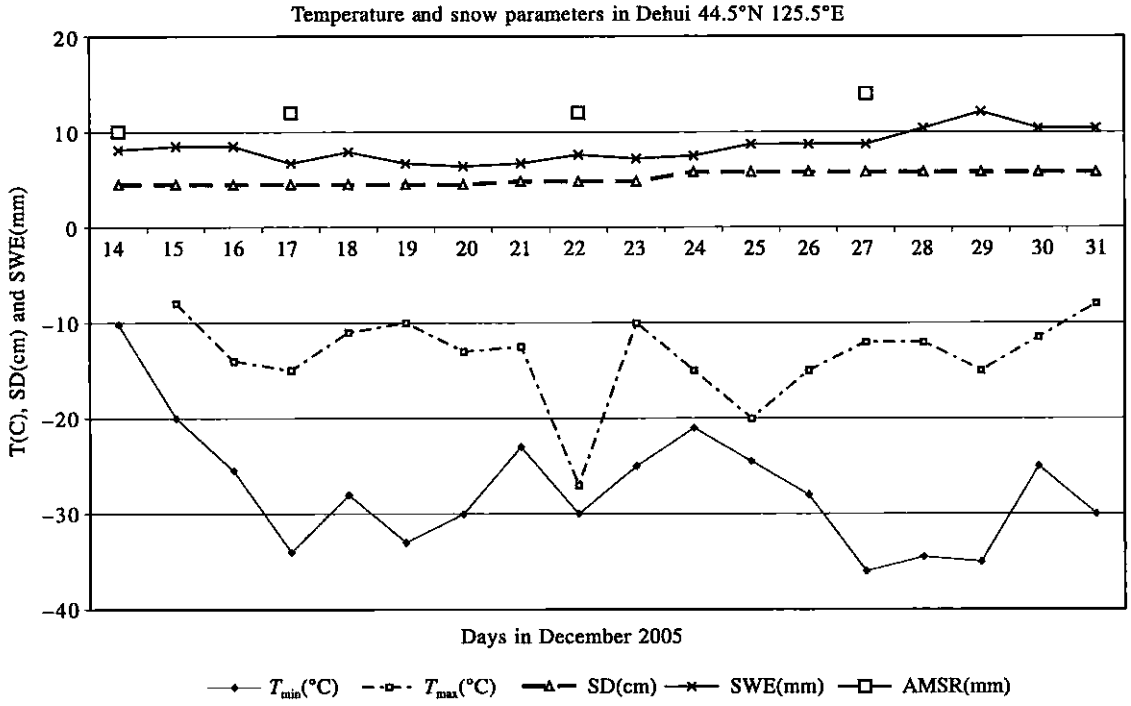

Figure 3. Same as Figure 2, except for station Dehui

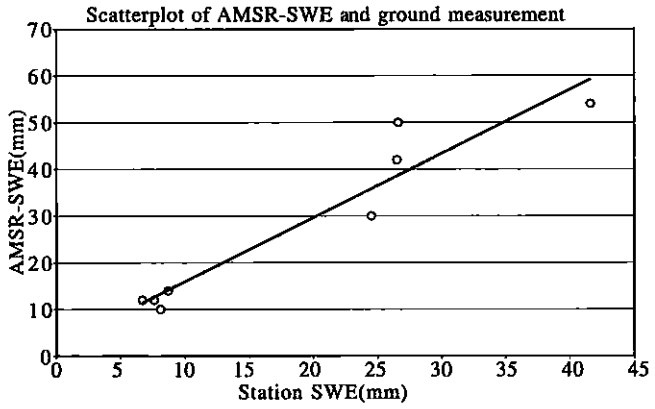

Figure 4. Scatterplot of AMSR-SWE vs. Station SWE for Qingyu and Dehui in December 2005

of measured SWE versus SWE derived from the Chang et al., algorithm (AMSR-SWE). The average measured and AMSR estimated SWE are 30.8 ±6.2 mm and 44 ± 9.1 mm for Qingyu and 8.4 ± 1.5 mm and 12 ± 1.4 mm for Dehui, respectively. The ± number indicates 1 standard deviation. The mean difference between the measured and AMSR-estimated SWE is 9.2 ± 6.8 mm. These statistics indicate roughly a 43% bias (AMSR estimates higher). Linear regression analysis show AMSR-SWE = 1.37*Station-SWE + 2.26 (all units in mm) with an R^2 value of 0.91. The correlation coefficient is significant at the 95%. However, there are only 8 samples. The data for Dehui are also clustered, effectively reducing the number of independent samples.

Monthly average conditions are examined next. The snow covered area (SCA) within a QuikSCAT pixel is determined from the pixel-wise percentage of snow covered ground (Hallikainen, et al., 2005).

$$SCA = \frac{\sigma_g^0 - \sigma_{obs}^0}{\sigma_g^0 - \sigma_{\min}^0} \times 100\% \quad (2)$$

where the subscripts g refers to snow-free ground, *obs* to observed value, and *min* to the minimum value for wet snow. The retrieval is based on a comparison of the backscattering cross section σ_0 against reference values for wet snow (minimum value at the onset of snowmelt) and snow-free ground (immediately after the end of snowmelt) (Koskinen, et al., 1997). The reference value for snow-free ground is obtained from the previous spring (Koskinen, et al., 1997; Hallikainen, et al., 2007). The main advantage of this method is that it allows real-time monitoring of SCA, since we do not need to wait until spring after snow melted to collect the reference value. In general, reliable determination of the two reference values is difficult due to daily variations attributed to weather conditions (Hallikainen, et al., 2005)

Table 2 shows the mean and standard deviation of scattering cross sections (equation 2). It can be noted that the mean difference in the numerator in Eq. (2) is very small. As a result, SCA is very sensitive to small errors in the reference values of snow free ground information. To improve the accuracy of reference value of snow free ground, detailed information of six county local weather stations have to be further examined.

Figure 5 and 6 show the SCA distribution maps from MODIS in Decembers 2005 and 2006, respectively. Visual inspection shows that the MODIS SCA maps are in reasonable qualitative agreement with the field data. In particular, the Muleng site

Table 2. Mean and standard deviation of scattering coefficients used in Eq. (1)

Orbit	Polarization	Mean$\left(\sigma_g^0-\sigma_{obs}^0\right)$dB	*Std deviation*$\left(\sigma_g^0-\sigma_{obs}^0\right)$dB
Ascending	H	1.81	0.31
Ascending	V	1.69	0.33
Descending	H	2.39	0.32
Descending	V	2.31	0.35

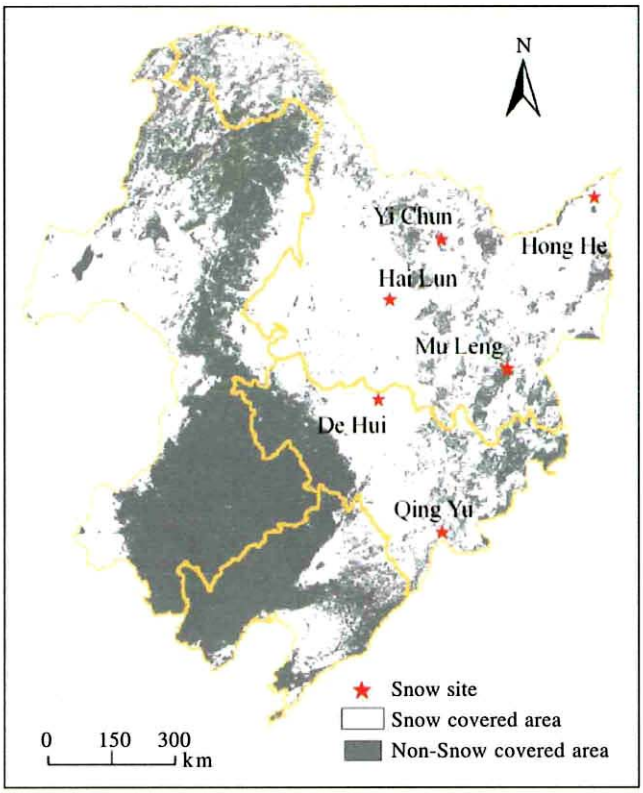

Figure 5. MODIS SCA in December 2005

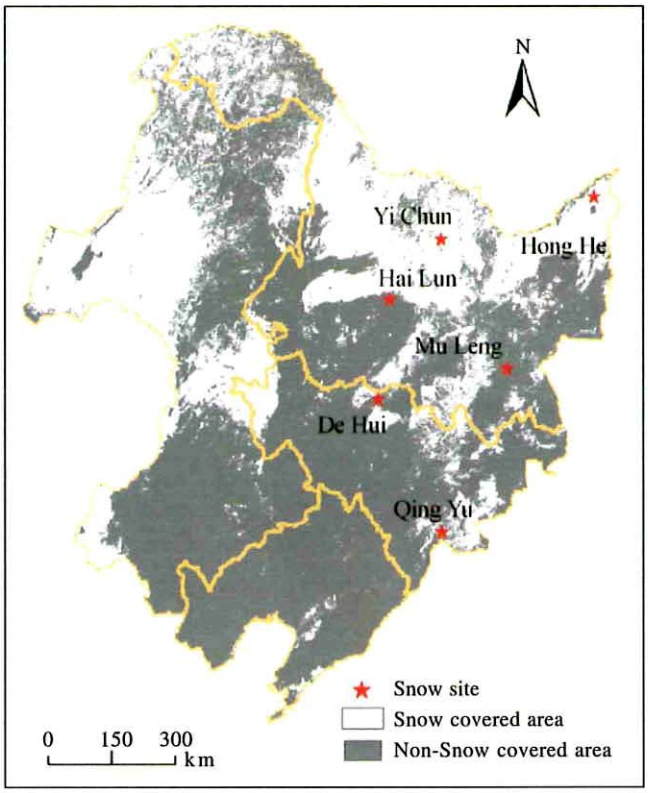

Figure 6. MODIS SCA in December 2006

shows almost no snow in December 2006, which is in qualitative agreement with the MODIS SCA estimate. It should be noted that snow free condition from MODIS SCA is a good indicator of no snow cover for the month since it indicates the maximum snow extent estimated, within the sampling error of MODIS.

Table 3 shows the averaged SWE of all six testing-sites estimated from AMSR-E data in Decembers 2005 and 2006. Figure 7 and 8 show the SWE distribution maps in Decembers of 2005 and 2006, respectively. They show a reasonable agreement with the field data.

The AMSR_SWE is higher for December 2005 than for December 2006, consistent with the results given in Table 3. In both years, the SWE in Qingyu, Yichun and Muleng are consistently higher than that in Dehui (Table 1 and Figures 7 and 8). It can thus be concluded that there is consistent spatial and temporal pattern of AMSR-estimated SWE and ground observations at the monthly scale.

IV. SUMMARY AND FUTURE WORK

The Chinese Academy of Science Northeast Institute of Geography and Agroecology launched a project to chart out the snow characteristics and monitoring snow variations in Northeast China. Two winters (2005–2006 and 2006–2007) of data have been acquired at six sites. Preliminary results show that satellite microwave sensors, such as QuikSCAT and AMSR-E can provide useful all-weather information of the snow field. SCA information generated from QuikSCAT is in qualitative agreement with high resolution MODIS SCA and they show reasonable agreement with the field data.

In this study, the results for December 2005 at two sites, Qingyu and Dehui, were presented. There are good agreement between AMSR estimated SWE and ground measurements (correlation coefficient of 0.9). The SWE estimated from AMSR is higher by about 43% compared to ground observation, which is

Table 3. The SWE estimated from AMSR-E data compared with field data in Decembers of 2005 and 2006

Years/SWE	Mean_measured	Mean_AMSR-E	RMSE(mm)	Error_relative	Correlation(r^2)
Dec2005	16.26mm	21.28mm	12.01	74%	0.54
Dec2006	8.7mm	17.00mm	10.01	115%	0.81

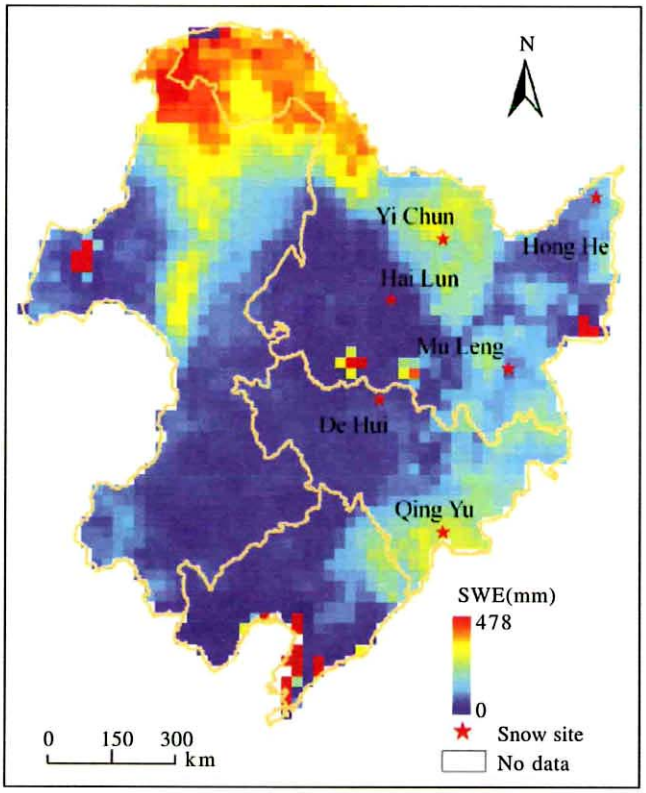

Figure 7. AMSR SWE map in December 2005

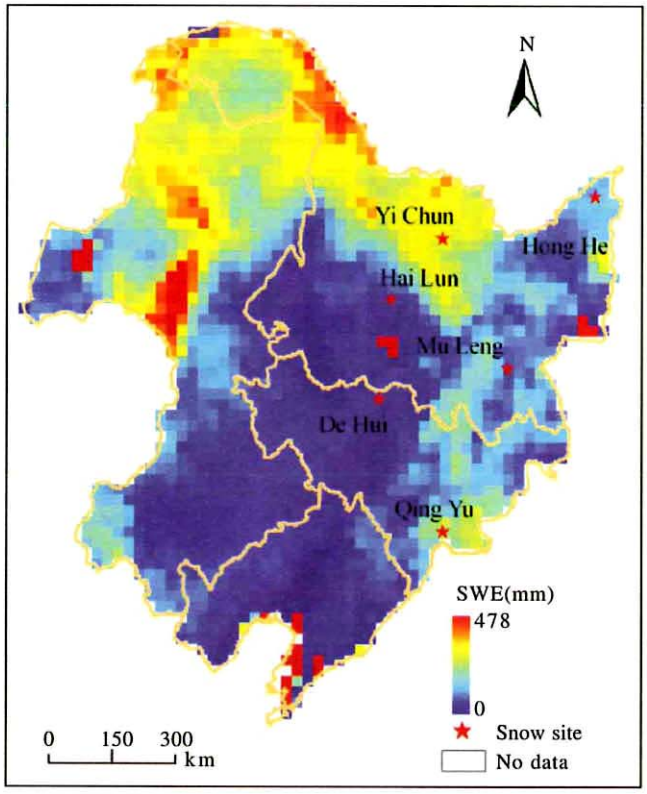

Figure 8. AMSR SWE map in December 2006

consistent with Tekeli (2008) and Derksen et al.'s (2005) results for the early snow season.

Tekeli (2008) examined the AMSR-E Level 3 EASE –grid SWE over Turkey and reported a cycle of over-estimation in the early snow season, turning to underestimation in the later half and finally back to over-estimation. The early over-estimation occurs at a snow density of less than roughly 0.25 g cm^{-3}, which can be compared to a snow density of <0.2 g cm^{-3} for Qingyu and Dehui in December 2005. Variation of the crystal radii and snow density may significantly change the assumptions in the global AMSR algorithm. In addition, stratification and texture in the snow greatly alter the microwave signature. Thus, to obtain more accurate SWE values from AMSR data, local density profiles as well as regional grain sizes should be used (Hall, et al., 2005). We plan to include information such as land surface type, daily maximum and minimum temperature, precipitation, snow properties such as density profile, grain size for the whole snow season data to make a full assessment of the utility of satellite remote sensing in snow monitoring in Northeast China.

ACKNOWLEDGMENTS

AMSR-E/Aqua L3 global SWE EASE-Grids data were provided by the National Snow and Ice Data Center in Boulder, Colorado. The MODIS SCA data are provided by NASA/Goddard Space Flight Center. QuikSCAT data are available from the PODAAC in JPL. The authors thank the support by the Knowledge Innovation Program of the Chinese Academy of Science (KZCX2-YW-340) and Direct Grants from the Chinese University of Hong Kong(2020970).

REFERENCES

[1] Bernier, M., J. Fortin, 1998, The potential of times series of C-band SAR data to monitor dry and shallow snow cover. *IEEE Trans. Geosci. Remote Sens.*, 36(1): 226–243.

[2] Chang, A. T. C., J. L. Foster, D. K. Hall, 1987, Nimbus-7 SMMR derived global snow cover parameters, *Annals of Glaciology*, 9, 39–44.

[3] Che, T., X. Li, F. Gao, 2004, Passive microwave remote sensing

retrieval of snow depth and snow water equivalent in Tibet-Qinghai Plateau. *Journal of Glaciology and Geocryology*, 26 (3): 261–266.

[4] Derksen C, Walker A, Goodison B, Strapp J., 2005, Integrating in situ and multi-scale passive microwave data for estimation of sub-grid scale snow water equivalent distribution and variability. IEEE Transactions on Geoscience and Remote Sensing, 43(5): 960–972.

[5] Foster, J. L., D. A. Robinson, D. K. Hall, T. W. Estilow, L. Chiu, 2008a, Spring snow melt timing and changes over Arctic lands. *Polar Geography,* Nov. 1–13.

[6] Foster, J. L., D. K. Hall, R. E. Kelly, L. Chiu, 2008b, Seasonal snow extent and snow mass in South America using SMMR and SSM/I passive microwave data (1979–2006). *Remote Sens. Environ.*, doi :10.1016/j.rse.2008.09010.

[7] Hall, D., et al., 2001, Algorithm Theoretic Basis Document for MODIS snow and sea ice mapping algorithm, NASA Goddard Space Flight Center, Greenbelt 20771 MD http://modis-snow-ice.gsfc.nasa.gov/atbd.html

[8] Hall DK, Kelly RE, Foster J, Chang AT, 2005, Estimation of snow extent and snow properties. In Encyclopedia of Hydrological Sciences, Volume 2 Part 5 Anderson MG (ed.); 811–830.

[9] Hallikainen, M., P. Lahtinen, Y. Zhang, M. Takala, J. Pulliainen, 2005, Feasibility of satellite Ku-band scatterometer data for retrieval of seasonal snow characteristics in Finland. *IEEE,* 1936–1939.

[10] Hallikainen, M., P. Sievinen, Y. Zhang, P. Halme, 2007, Use of QuikScat Ku-band Scatterometer data for retrieval of seasonal snow characteristics in Finland. *IEEE,* 1228.

[11] Kelly, R. E. J., Alfred T. C. Chang, James L. Foster, Marco Tedesco, 2004, updated every five days. *AMSR-E/Aqua 5-day 3 Global Snow Water Equivalent EASE-Grids* V002, [December 2005]. Boulder, Colorado USA: National Snow and Ice Data Center. Digital media.

[12] Koskinen, J., S. Metsämäki, J. Grandell, S. Jänne, L. Matikainen, M. Hallikainen, 1999, Snow monitoring using radar and optical satellite data, *Remote Sensing of Environment*, 69(1): 16–29.

[13] Liang, T., X. Huang, C. Wu, X. Liu, W. Li, Z. Guo, J. Ren, 2008, An application of MODIS data to snow cover monitoring in a pastoral area: A case study in Northern Xinjiang, China. *Remote Sens. Environ.,* 112(4): 1514–1526.

[14] Nghiem, S. V., K. Steffen, G. Neumann, R. Huff, 2008, Snow accumulation and snowmelt monitoring in Greenland and Antarctica, *Chapter,* 5, 31–38.

[15] Parajka, J., G. Bloschl, 2008, The value of MODIS snow cover data in validating and calibrating conceptual hydrologic models. *Journal of Hydrology*, 358: 240–258.

[16] Pulliainen, J., 2006, Mapping of snow water equivalent and snow depth in boreal and sub-article zones by assimilation space-borne microwave radiometer data and ground-based observations. *Remote Sens. Environ.,* 101(1): 257–269.

[17] Rott, H, and T. Nagler, 1994, Intercomparison of snow retrieval algorithms by means of spaceborne microwave radiometry, in Passive Microwave Remote Sensing of Land-Atmosphere Interactions, Choudhury, B.J, Y. H. Kerr, E. G. Njoku, and P. Pampaloni., (Eds), Utrecht, the Netherlands, 227–243.

[18] Song, K. S., Y. Zhang, 2008, Snow-cover environmental monitoring and assessment in Northeast China using passive microwave emission models. *Environ. Monitor. Assess.,* 140(1–3): 223–229.

[19] Tekeli, A. E., A. Zuhal, S. Arda, S. Aynur, S. Unal, 2005: Using MODIS snow cover maps in modeling snowmelt runoff process in the eastern part of Turkey. *Remote Sens. Environ.,* 97: 216–230.

[20] Tekeli, A. E., 2008, Early findings in comparison of AMSR-E/Aqua L3 global snow water equivalent EASE-grids data with in situ observations for Eastern Turkey. *Hydrol. Process.* 22, 2737–2747

[21] Wang, X., H. Xie, T. Liang, 2008, Evaluation of MODIS snow cover and cloud mask and its application in Northern Xinjiang, China. *Remote Sens. Environ.*, 112(4): 1497–1513.